1

Heavy metallic concentration in microbial mats found at hydrothermal systems, Kamchatka, Russia

Kazue TAZAKI[1], Victor OKRUGIN[2], Masayuki OKUNO[1], Natalia BELKOVA[3],
ABM Rafiqul ISLAM[3], S. Khodijah CHAERUN[3], Rie WAKIMOTO[3],
Kazuhiro SATO[3], and Shingo MORIICHI[1]

1 Department of Earth Sciences, Faculty of Science, Kanazawa University, Kakuma, Kanazawa, 920-1192 Japan

2 Institute of Volcanology Far Eastern Division of Russian Academy of Sciences, 9 st. Piip, Petropavlovsk-Kamchatskii 683006 Russia

3 Graduate School of Natural Science and Technology, Kanazawa University, Kakuma, Kanazawa, 920-1192 Japan

Abstract : This study described the investigation of microbial mats that are rich in iron, arsenic, and manganese in four hydrothermal systems of Kamchatka, Russia namely Vilyuchinskie, Mutnovskie, Nachikinskie, and Malkinskie. The hydrothermal systems (hot springs) are contributing to the metallic and non-metallic mineral resources of Russia such as oil, gas, coal, copper, nickel, cobalt, tin, mercury, lead, zinc, diamond, platinum, gold, and silver. We observed the biogeochemical activities of microorganisms originating from microbial mats. The structure and elemental composition of microbial mats in these hydrothermal systems were studied with optical microscopy and scanning electron microscopy equipped with energy dispersive X-ray analyzer (EDX), whereas the water quality of these springs was measured by using pack tests. Additionally, portable γ-ray analyzer was employed to determine the kind and quantity of γ-ray in the atmospheric condition of sampling areas. Optical and scanning electron microscopic observations revealed that the microbial mats at these springs were mainly composed of a large number of microorganisms such as bacteria (coccus, bacillus, and filamentous), cyanobacteria, and algae in association with biominerals. Bacterial fluorometric enumeration of the thermal water informed that the total number of bacteria was relatively low, while the fraction of enzymatically active bacteria was high ranging from 27 % to 91 %. Besides that, γ-ray observation showed that the predominantly γ-ray range was between 320～380 keV dominating in green and black-colored microbial mats at Vilyuchinskie hot springs. Correspondingly, heavy metal and minerals deposits accumulated at all these springs indicating that microorganisms may contribute to binding and formation of the minerals. These activities and heavy mineral encrustation of cyanobacteria, bacteria, and algae may contribute to the growth of the heavy metal deposit (such as iron, manganese, and arsenic) at these springs. Obviously, Kamchatka hot springs provide a model for studying the potential role of prokaryotes and eukaryotes in the origin of heavy metal and minerals formation.

Keywords : microbial mats, microorganisms, heavy metals, arsenic, manganese, iron, γ-ray, hydrothermal systems, Kamchatka, Russia.

1. Introduction

The Kamchatka Peninsula is a part of the Pacific rim of fire and the only example of modern volcanic activity in Russia. The volcanic history of the Kamchatka Peninsula goes back to the Cretaceous (130~140 m.y.) and still continues, resulting in several long volcanic belts (Okrugin, 1995). The Kamchatka Peninsula is a typical arc-trench system of the circum-pacific belt, where the Pacific plate is being subducted westward beneath the Asian continent. As a result, four roughly parallel, N-S oriented, volcanic mountain chains were formed (Lattanzi *et al* ., 1995). Kamchatka is rich in several metallic and non-metallic minerals including oil, gas, coal, copper, nickel, cobalt, tin, mercury, lead, zinc, diamonds, platinum, gold, and silver (Okrugin, 1995). About 75 % of hydrothermal and mineral water resources of Russia are concentrated in Kamchatka. Over 150 groups of hot springs occur in four geothermal provinces. Hot springs and geothermal systems are not only the source of geothermal energy, but also the habitat of microorganisms. In view of the fact, that researches of these unique ecological systems have been started not far ago. However, only little is known about microorganisms in these modern geothermal systems. Likewise, no one has ever touched upon the problem of biomineralization with heavy metals and radioactive materials in these geothermal systems of Kamchatka.

One of four geothermal provinces known as the Southern-Kamchatskaya province or the South-Kamchatka mining area is located in the southward of Petropavlovsk, the capital city of Kamchatka (Fig. 1), to Lopatka cape. This area is characterized by diverse volcanic, hydrothermal and ore-forming (metallogenic) activities. The great reserves of gold-silver ores and geothermal heat of the South-Kamchatka mining area are located there. Such deposits as Asachinskoe, Mutnovskoe, and Rodnikovoe epithermal deposits of gold and silver with reserves Au > 100 t, Ag > 10000 t, and a considerable number of different ore manifestations were formed there. They show a distinct relationship between mercury aureoles and zones of gold-silver mineralization (Takahashi *et al* ., 2001 ; Stepanov *et al* ., 2001). Mercury is an effective indicator of hydrothermal-type (epithermal) ore deposits. Studying heavy metal deposits associated with microorganisms by which the element was taken from hot springs in the hydrothermal systems, is particularly informative.

It has been well known that the widespread bacterial mineralization of metallic ions contributes to immobilization of mineral-forming elements through a continuum of reactions involving sorption and mineral precipitation in hot springs (Tazaki, 1997 ; Tazaki *et al* ., 1998 ; Tazaki, 1999 ; Tazaki, 2000). Yet, despite its enormous economic significance and hundreds of research papers over past decades, no consensus has been reached on the origin of the gold suggesting two models of (1) sedimentary places and (2) a hydrothermal model (Frimmel, 2002). Moreover, none of research papers described biomineralization of gold, silver, and radioactive materials in natural environments. It was also reported that Fe (III)−reducing bacteria and Archaea were some of these organisms capable of precipitating gold by reducing Au (III) to Au (0) with hydrogen as the electron donor (Kashefi *et al* ., 2001). Thereby, these studies suggested that models for the formation of gold deposits

in hydrothermal systems should consider the possibility where dissimilatory metal-reducing microorganisms can reductively precipitate gold from hot springs.

Additionally, thermoacidophilic microorganisms isolated from the acid hot springs of Kamchatka, Muntovskii volcano, Geyser valley, and Uzon caldera, were studied (Prokofeva *et al*., 2000). These investigations showed that obligatory anaerobic organisms with fermentative metabolism are widespread in Kamchatka hot springs with low pH. However, hot springs with neutral pH and high mineralization are abundant among hydrothermal areas of Kamchatka Peninsula. All of them attract attention to high concentrations of heavy metals in water, such as Sr and Cr (Paratunskie and Malkinskie hot springs), As and Cd (Vilyuchinskie hot springs), Cd (Mutnovsky geothermal field) (Okrugin *et al*., 1994 ; Aoki *et al*., 1998 ; Chudaev *et al*., 2000).

In 2002 on October 5～16 [th], we have visited four hydrothermal systems of Southern and Central-Kamchatka mining regions (provinces), such as Vilyuchinskie, Mutnovskie, Nachikinskie, and Malkinskie, which are characterized by a diverse hydrothermal activity under high temperature systems (Mutnovskie is high temperature hydrothermal system, while others are low temperature ones).

In this study, the high concentrations of Mn, Fe, As, and radioactive materials related with microbial mats in hot springs and hydrothermal systems have been found. The results could provide opportunities for the investigation of not only ore minerals, but also organic mineral formation processes (biomineralization). The microbiological observation in this study indicates that bacteria and archaea are capable of long-term persistence and high activity in the hydrothermal systems. As well, to our knowledge this is the first time investigation of microscopic and chemical analyses of microbial mats consisting of microorganisms in association with ambient γ-ray analysis at the high and low temperature hydrothermal systems of Kamchatka has been reported.

2. Geological setting

In geological terms Kamchatka is one of the poorest studied regions of Russia. Unfortunately, there are no recognized and accepted by the majority of geologists schemes (charts) of tectonic, geological, metallogenic, hydrogeological, and mining divisions into districts (there is still no common classification for all schemes/charts). Thus, in mining and metallogenic terms there are two metallogenic provinces and three mining regions here (these terms and notions are used by metallogenists and economical geologists). Hydrogeologists speak about four geothermal provinces (Northern-Kamchatskaya, Sredinno-Kamchatskaya, Eastern-Kamchatskaya, and Southern-Kamchatskaya) and five geothermal areas (Pauzhetskaya, Mutnovskaya, Paratunskaya, Semyachinskaya, Kireunskaya) which include 23 or as many as 24 hydrothermal systems of high and low temperatures (Kiryukhin and Sugrobov, 1987 ; Okrugin *et al*., 2002).

Vilyuchinskaya hydrothermal system is located between Northern-Mutnovskaya and Zhirovskaya high-temperature in the south and Paratunskaya low-temperature hydrother-

mal systems and Vilyuchinskii and Zhirovskoi volcanoes of upper-Pliestocene-Holocene age in the north. It is located $55\sim60$ km southward of the town Petropavlovsk-Kamchatskii in the area of the Vilyucha and the Bystraya rivers. Host rocks are Oligocene (volcanogenic-sedimentary and volcanogenic formations), Pliocene (subvolcanic and intrusive diorites) to Holocene (Vilyuchinskii volcano andesites and extrusive liparites). Natural plots of thermal waters (on the surface) are orientated (traced, stretched) mainly in latitudinal direction on both banks of the Vilyucha river as narrow strikes ($50\sim150$ m wide) about 3 km long. They form four groups. The most high-temperature one was discovered by prospecting of Rodnikovoe epithermal gold-silver deposit (adit 1, Temp. $= 78\sim93$ ℃) and by bore-holes on the right bank of the Spokoynyi brook ($55\sim78$ ℃). Hydrogeological bore-hole 2, drilled on the travertine terrace, at a depth of $31.5\sim234$ m met a water-bearing gushing horizon in diorites with temperature of 78 ℃. The second bore-hole, drilled 70 m eastward, enabled to discover thermal waters with temperature of $55\sim56$ ℃. The third and largest group of springs called Travertine dome or Karbonatny dome is located 500 m eastward on the right bank of the Vilyucha river. Waters of all springs have a similar chemical composition. These are hydrocarbon-sodium neutral waters with mineralization up to 1.5 g/l. Vapor composition of waters is carbonic-acid-nitrous ($N_2 = 66$ % vol., $CO_2 = 32$ % vol.) with temperature of 95 ℃.

Mutnovskaya hydrothermal system belongs to Mutnovskii geothermal area which is located $70\sim75$ km southward of the town Petropavlovsk-Kamchatskii, between active volcanoes Mutnovskii (in the south) and Gorelyi (in the west). It is located in the graben zone or in the tectonic hollow formed by a series of submeridional faults that are altogether called Northern-Mutnovskaya volcanic-tectonic zone. It is characterized by numerous Pleistocene-Holocene extrusions, scoria cones, and natural vapor-steam jets-springs of different sizes/scale. In addition, some scientists speak about Northern-Mutnovskaya and Zhirovskaya hydrothermal systems in the structure of Mutnovskii geothermal field (Vakin, *et al*., 1977). Lately it acquired a name of Northern-Mutnovskoe geothermal field (Kiryukhin, 2002). On this territory (Mutnovskaya hydrothermal system) there are the following groups of thermal manifestations and hydrothermal springs (located from south to north)： Northern crater and Active crater of Mutnovskii volcano, Northern-Mutnovskie Eastern, Northern-Mutnovskie Western, Dachnye and Perevalnye (Kiryukhin and Sugrobov, 1987). The most ancient rocks (Oligocene) of the system are volcanogenic-sedimentary and volcanogenic deposits (sandstones, conglomerates, aleuroites, tuffs, and lavas of andesites, dacites, ignimbrites) forming the basement. Upper or the youngest middle-upper-Pleistocene parts of geological section are effusive, extrusive, and pyroclastic facies from andesite-dacites to liparites. We visited only one thermal plot that belongs to Dachnye springs, called Active group. Mutnovskaya and Vilyuchinskaya hydrothermal systems belong to one Southern-Kamchatskaya geothermal province and to different geothermal regions called Mutnovskie and Paratunskie (Vilyuchinskie).

Nachikinskaya hydrothermal system is located $85\sim90$ km northward of the town

Petropavlovsk-Kamchatskii in the valley of rivers the Avacha, the Plotnikova and the Bystraya. It belongs to Eastern-Kamchatskaya geothermal province. According to the hydrogeological terms, it is located in the zone of Sredinnyi massif of Kamchatka. Host rocks are Cretaceous-Paleogene vulcanites (kirganikskaya suite), intruded by Miocene granodiorites. They are blocked by a cover (coat) of loose Quaternary deposits (alluvial formations, fluvio-glacial deposits) up to 35 m in thickness. These deposits of the lower part of the section are characterized by low permeability (they are cemented) and are a good waters-bearing horizon. In zones of increased fracturing, connected with diagonal fractures of north-eastern and north-western strikes, there is circulation of hot thermal waters and heat. It was also studied by drilling of hydrogeological bore-holes (50～360 m deep) where temperature of water at these depths is from 80 ℃ up to 85 ℃. By chemical composition, thermal-mineral waters are chloride-sulfate-sodium from neutral to alkaline (pH = 6.3～8.5), mineralization is 0.45～1.25 g/l, siliceous (H_2SiO_3 ; 50～180 mg/l), also they contain fluorine of 1.8 to 4.0 mg/l. Mineral new formations (deposits from hydrothermal on sides of bore-holes, tubes, and diorite fragments) consist of chlorides and sulfates of sodium, potassium, and iron. The water temperature generally ranges between 75 ℃ and 80 ℃, while at a depth of 1500 m is up to 96 ℃.

Malkinskaya hydrothermal system is one of the most widely known geothermal objects in Kamchatka. It is located near the settlement Malka on the 125 km from the Petropavlovsk-Milkovo. Malkinskie thermal springs are one of the most popular and favourite places of rest among inhabitants of Kamchatka. They are located at the central Kamchatka region in the valley of rivers of the Avacha, the Plotnikova and the Klyuchevka and do not belong to any of four known geothermal provinces. In geological terms this hydrothermal system is localized in the eastern part of Sredinny massif of Kamchatka formed by ancient metamorphic rocks. Host rocks are presented by metamorphic schists, volcanogenic and volcanogenic-sedimentary deposits (lavas, tuffs, tuff-breccias) of basic and intermediate composition. They are upper-Cretaceous and intruded by numerous dykes, subvolcanic intrusive bodies of basic and acid composition from late-Cretaceous to late-Miocene. They are blocked by a thick cover (20～30 m to 90 m) of modern (Quaternary) loose deposits from the surface. Besides this, two-layer structure is the water-bearing complexes of different ages. These are Quaternary alluvial-water-glacial complex and upper Cretaceous-Neogene complex of volcanogenic-siliceous and intrusive rocks. The deposit is well studied by bore-holes up to 1522 m deep. The main thermal-productive zones (water-bearing horizons) are at depths of 650～750 m to 1500 m. Waters are neutral to slightly alkaline (pH is 7.8～9.7) with the maximum temperature of 92.4 ℃.

3. Materials and Methods

3.1. Sampling and field measurements of water quality and γ-ray values

Samples of microbial mats, hot spring water, sediments, and rocks were collected from four hydrothermal fields of South and Central Kamchatka provinces namely Vilyuchinskie, Mutnovskie (Dachnye), Malkinskie, and Nachikinskie hot springs on 8～14th of October, 2002 (Fig. 1, 2, 3, 4, 5, 6). Measurement of chemical characteristics of hot spring water (pH, Eh, EC, DO, and WT) was done in the field (Eh : Electrode potential versus the standard hydrogen electrode, EC : Electrical conductivity, DO : Dissolved oxygen, WT : Water temperature). Concentrations of elements, such as Mg, Ca, Fe^{2+}, total Fe, As, Ag, and Au in hot spring waters were detected at on-site by using pack-tests (Kyoritsu Chemical-Check Lab.). Values of γ-ray were measured by using two types of γ-ray counters : Spectrosurvey meter (SSM ; Hamamatsu : C 3475) and Radi (HORIBA : PA-300). Before measuring with SSM, analyzer was calibrated with ^{40}K standard. Measurements were conducted within 5 min. Spectrum of total γ-ray were detected and values of isotopes ^{141}Ce, ^{131}I, ^{103}Ru, ^{137}Cs, ^{60}Co, ^{40}K (energy ranged between 50 keV～1670 keV) and total γ-ray were calculated. Additional measurement of total γ-ray values was undertaken with portable γ-ray counter Radi. Measurements were carried out 3 times for 2 min. for determination of average values.

3.2. Energy dispersive X-ray fluorescence analysis (ED-XRF)

Fresh microbial mats and sediment samples were air-dried up at room temperature and ground to fine powder for ED-XRF analysis. The powder samples were pressed to make pellet and mounted on the Mylar film. Analysis was carried out by an energy dispersive X-ray fluorescence spectrometer (JEOL JSX-3201), using Rh Kα, which operated at an accelerating voltage of 30 kV under a vacuum condition.

3.3. X-ray powder diffractometer (XRD)

The powder material was mounted onto slide glasses to fit the diffractometer sample-holder. To ensure accurate clay mineral identification and characterization of clay particles, separation of clays (< 2 μm) from silt fractions was made by centrifugation (Kokusan : H-26 F), and the obtained slurry of < 2 μm was sedimented and dried on a glass slide. X-ray diffraction analyses of bulk samples and < 2 μm oriented samples, which comprise untreated, ethylene glycol-treated and thermally-treated clay specimens, were carried out using a Rigaku RINT 1200 X-ray diffractometer with a CuKα radiation, generated at 40 kV and 30 mA and scanned speed of $2^{°}$/min.

3.4. Fluorometric enumeration of bacteria in the hot spring waters

Two fluorometric methods were used for bacteria counting procedures (Miskin *et al*., 1998). Samples of hot spring waters were fixed immediately after collection either with 1% glutaraldehyde for total bacteria number or with 0.1 mM 5-carboxyfluorescein diacetate

(CFDA) for enzymatically active bacteria counting. All samples were incubated statically at 10 ℃ until required for microscopic observation. In the laboratory, 4',6-diamidino-2-phenilindole (DAPI) was added to glutaraldehyde fixed water samples, at a final concentration of 0.5 μg/ml in solution and stained for 5 min. In both cases, each sample was filtrated through 0.22 μm black membrane filter, washed with bacteria-free water and stored in the dark before counting for 20 min. Negative controls comprised autoclaved samples.

Furthermore, filters were wet mounted onto slide glasses with low-fluorescence immersion oil and counted within 20 min after staining. Stained cells were visualized with epifluorescence microscope (Nikon EFD-3) by using the appropriate optical filters and 100× Plan objectives. For each sample, more than 500 cells were enumerated. In addition, the fraction of enzymatically active bacteria (EAB) were calculated as the product of their relative abundances on the filter and the DAPI-stained direct cell counts. The mean abundances and standard deviations (SD) were calculated from the counts of 10 to 20 fields chosen randomly for each scanned-filter.

3.5. Optical light and epifluorescence microscopy of hot spring microbial mats and sediments

Microbial mats and sediments from hot springs were fixed with 2.5 % glutaraldehyde in the field and stored at 10 ℃ until required for microscopic observation. Fixed samples were stained with DAPI (5 μg/ml) for 3 min. to observe under epifluorescence microscope (Nikon EFD-3 ; Digital camera : Nikon COOLPIX E 995). For epifluorescence microscopy, a filter UV-1 A wavelength of exposed light : 360～370 nm) was used for DAPI-staining observation and a filter G-2 A (wavelength of exposed light : 510～560 nm) for chlorophyll observation.

3.6. Scanning electron microscopy (SEM-EDX)

Freeze-dried method was used for sample preparation (Suzuki *et al* ., 1995). One drop of fixed microbial mats was mounted onto JEOL filter, sample was then washed and fixed with *t*-butyl alcohol, frozen in liquid nitrogen and dried up with low-vacuum SEM. After the completion of freeze-drying, the sample was transferred on cupper-stub with double-sided adhesive carbon tape, coated with carbon and observed with a scanning electron microscope (JEOL JSM-5200 LV), equipped with an energy dispersive X-ray spectrometer (Philips-EDX PV 9800 STD).
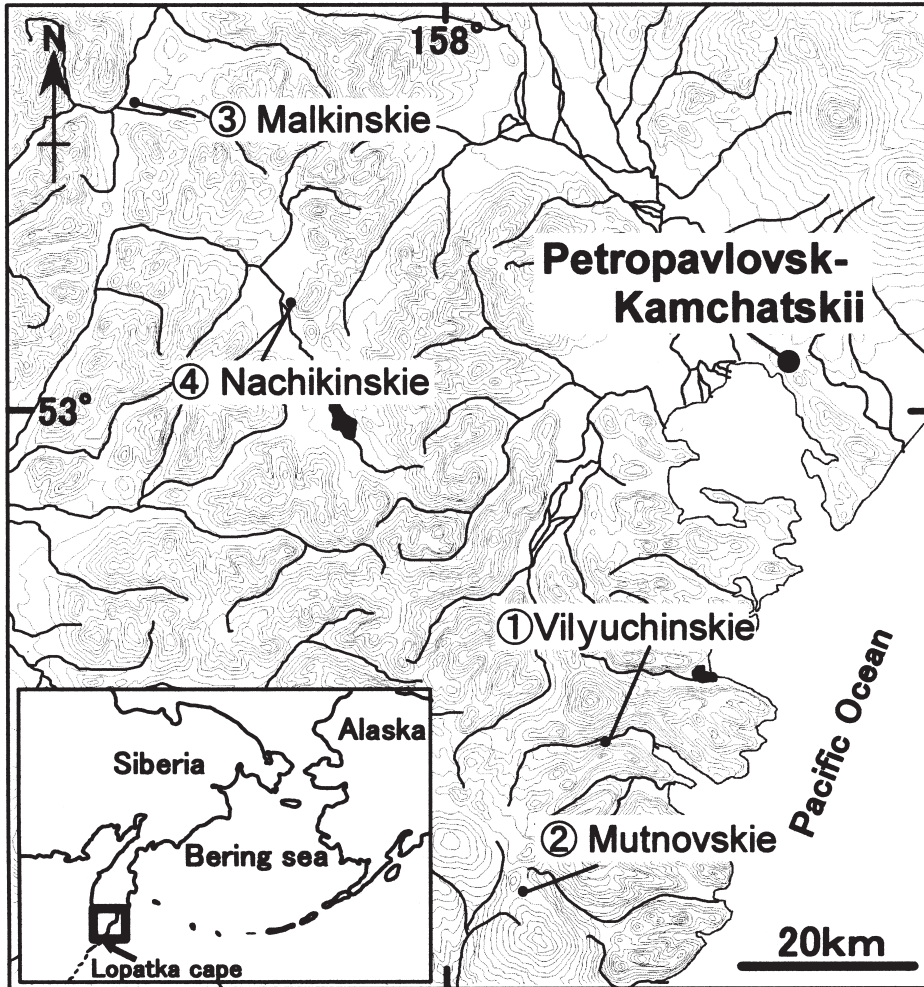
Fig. 1. Location map of Vilyuchinskie ① (V), Mutnovskie ② (M), Malkinskie ③ (Ma) and Nachikinskie ④ (N) hot springs in Kamchatka (Southern and Central parts near Lopatka cape), Russia.

Fig. 2. Field views of sampling and measuring points at Vilyuchinskie hot springs (location ①) (V) in Southern Kamchatka, Russia (8th, October, 2002). V 1 ; Reddish brown microbial mats predominated in the hot spring stream. V 2 ; Green microbial mats in a wetland. V 3 ; Reddish brown microbial mats formed in the hot spring steam from bore-holes N 1. V 4 ; Black microbial mats formed near to the outlet of waterflow from adit 1, Rodnikovoe epithermal deposit. Sampling points are marked by arrows.
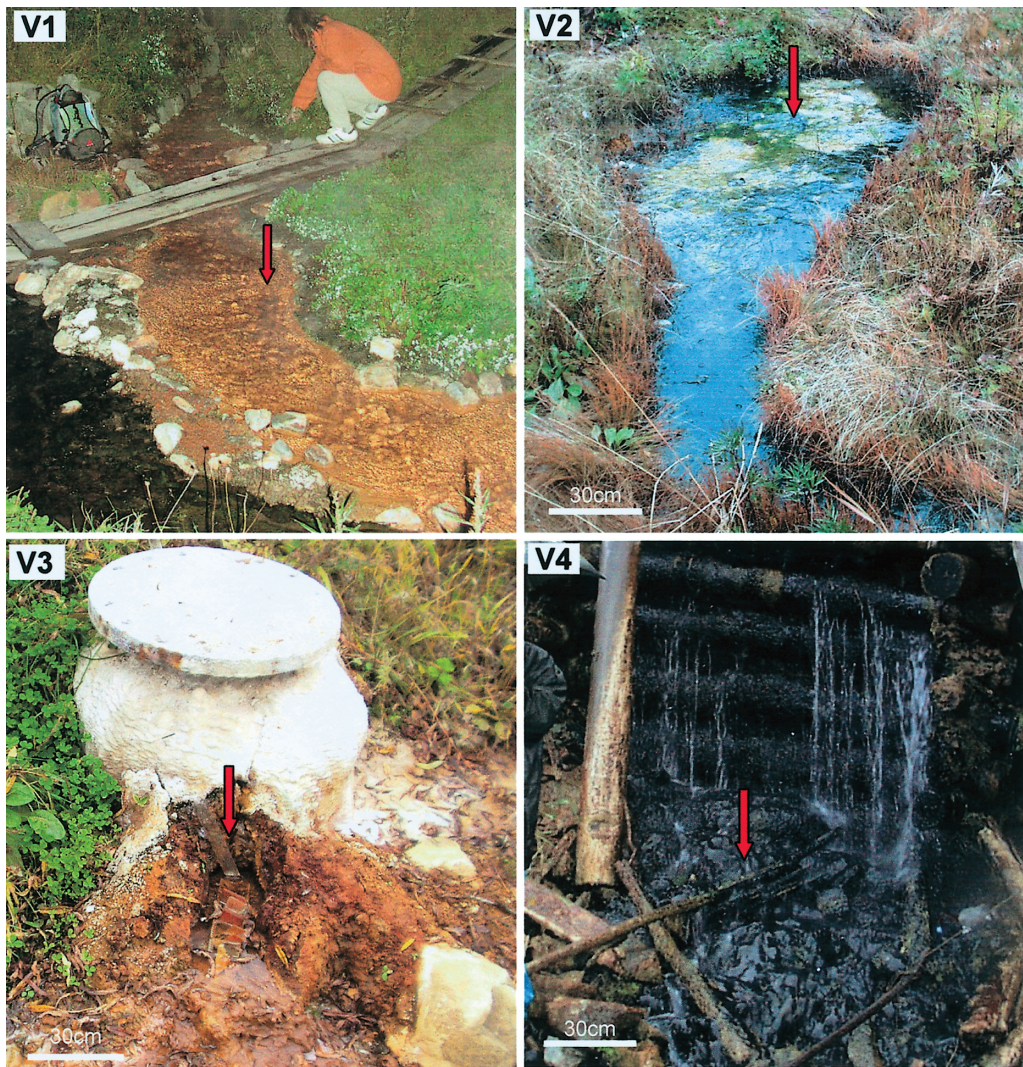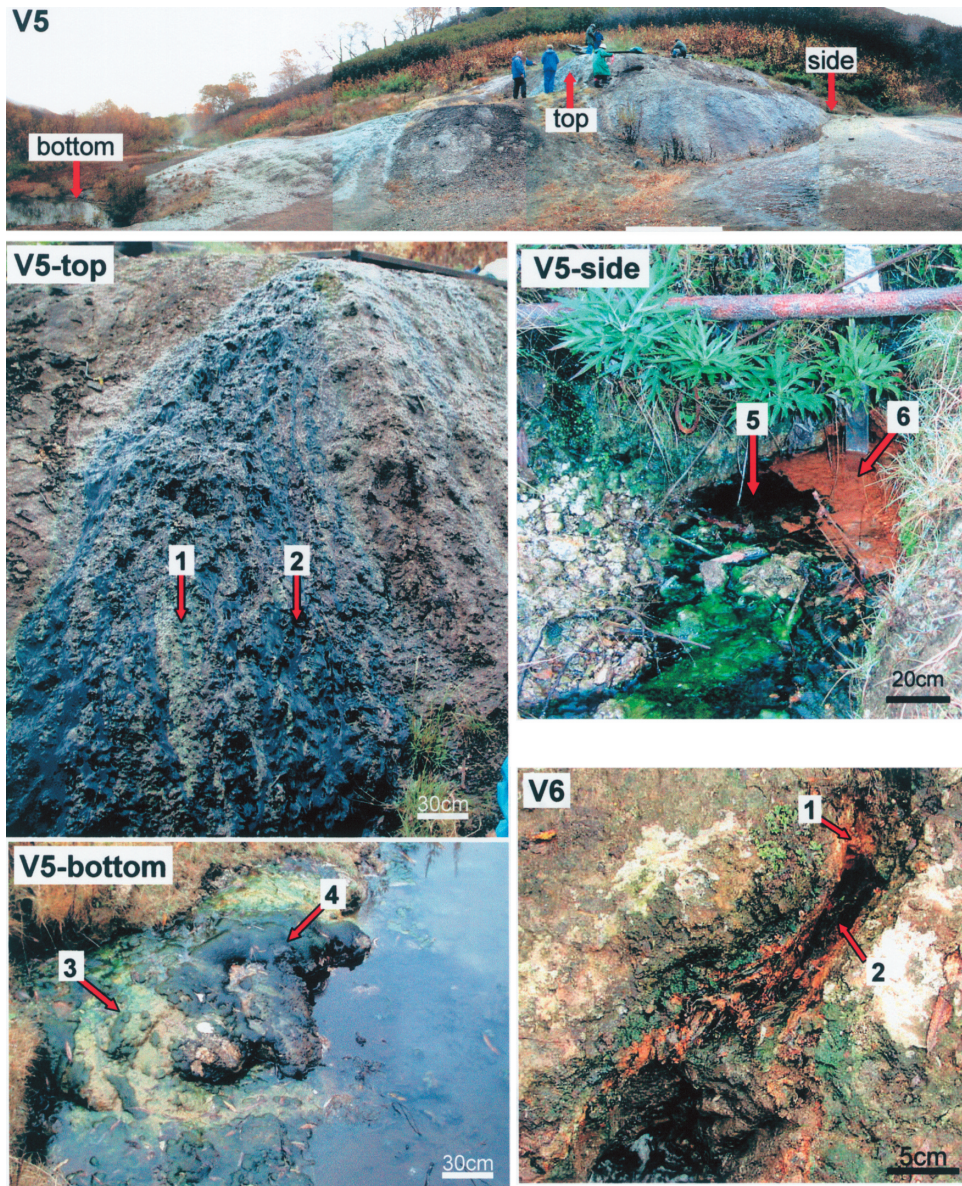
Fig. 3. Field views of sampling and measuring points at Vilyuchinskie hot springs (location ①) (V) in Southern Kamchatka , Russia (8 th, October, 2002). V 5 ; general view of travertine dome and terrace. V 5-top ; Green (1) and black (2) microbial mats formed on the top of the travertine dome. V 5-bottom ; Green (3) and black (4) microbial mats formed in the pond at the bottom of travertine dome. V 5-side ; source of natural hot springs beside travertine dome with green (5) and red-colored (6) microbial mats. V 6 ; red-colored microbial mats (1) and black-colored sediments (2) from arsenic-rich hot springs. Sampling points are marked by arrows.
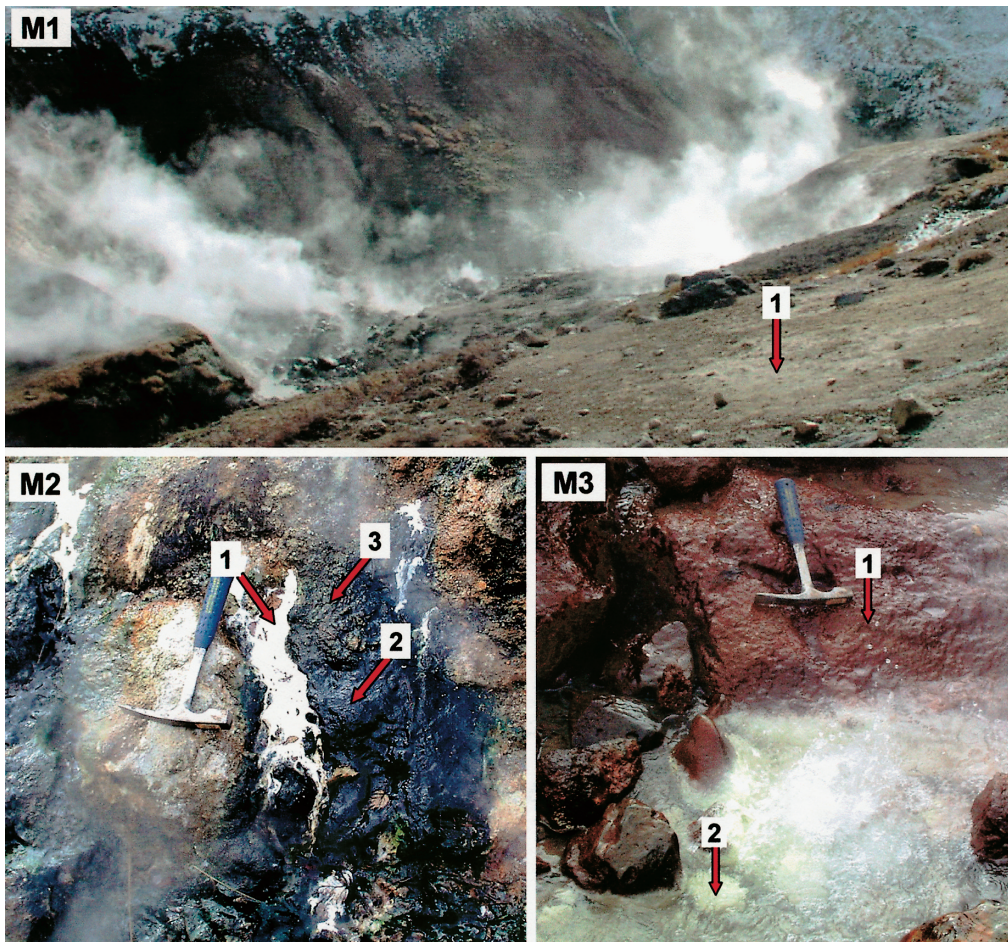
Fig. 4. Field views of 3 spouts (M 1～M 3) with arrow marks showing the sampling and measuring points at Mutnovskie hot spring (Active group) (location ②) (M), Mutnovskie geothermal field in Southern Kamchatka, Russia (10 th, October, 2002). M 1 ; general view of Mutnovskie hot springs with soil sampling point (1). M 2 ; white (1), green (2), and grey (3) microbial mats in a hot spring waterflow. M 3 ; Brown (1) and white (2) rocks around the waterflow of different source in the same Mutnovskie hydrothermal field. Sampling points are marked by arrows.

Fig. 5. Field view of 3 spouts (Ma 1 〜 Ma 3) with arrow marks showing the sampling and measuring points at Malkinskie hot springs with its general view at location ③ (Ma) in Central Kamchatka (12 th, October, 2002). Ma ; General view of sampling spouts in Malkinskie hot springs area beside the Malka river. Ma 1 ; Green (1) and orange (2) microbial mats formed around the hot spring water reservoir. Ma 2 ; Black (3) and brown (4) microbial mats formed on the stream towards the reservoir. Ma 3 ; White (5) and grey (6) microbial mats formed on the other stream towards the same reservoir. Sampling points are marked by arrows.
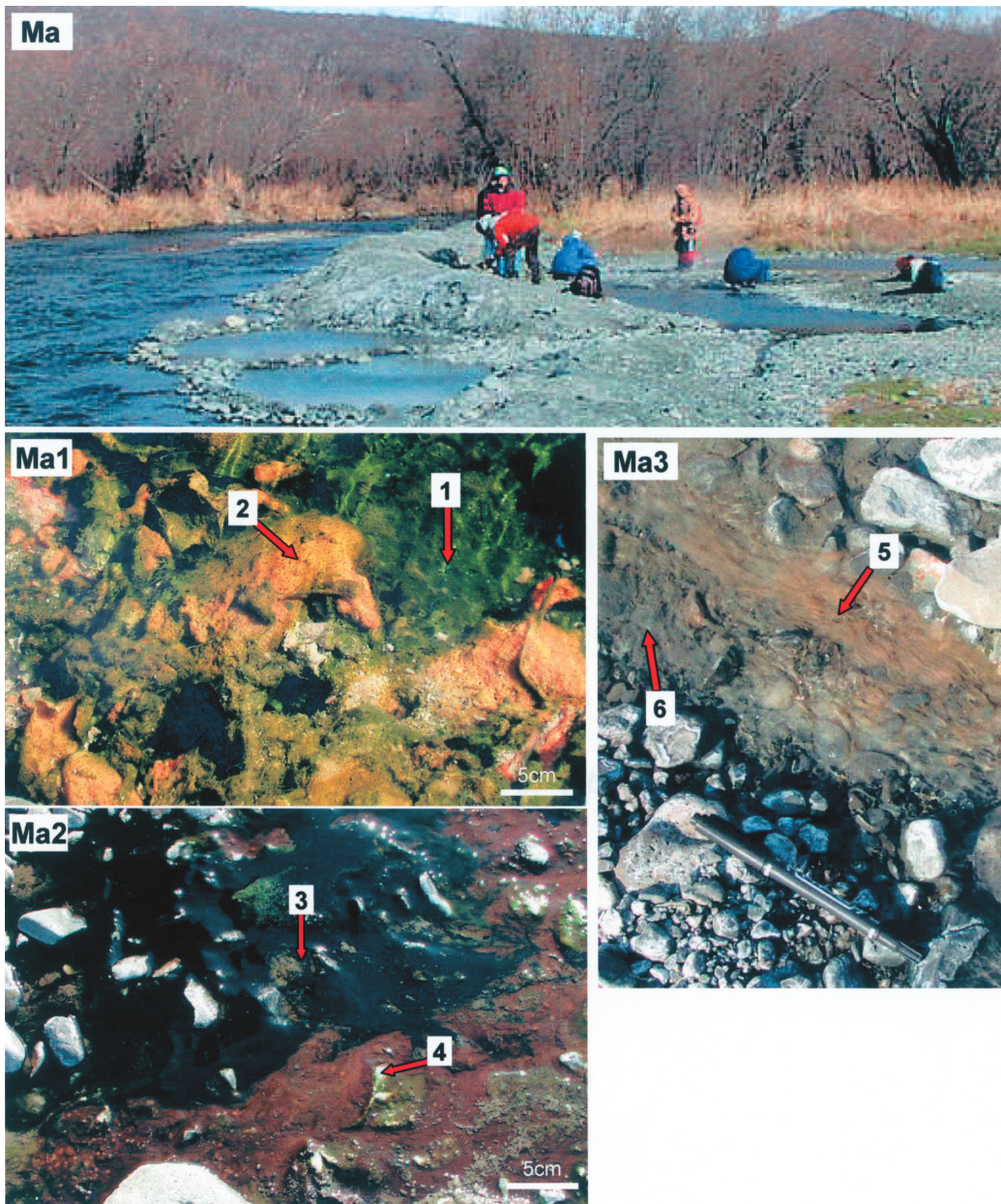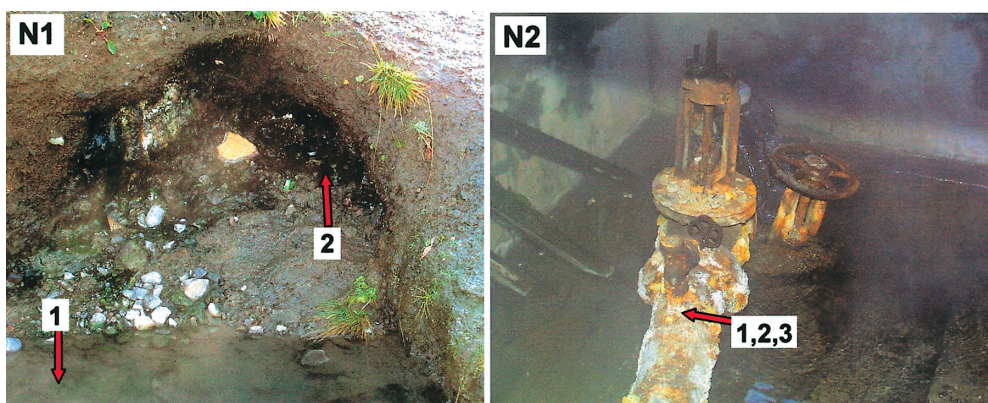
Fig. 6. Field view of 2 spouts (N 1〜N 2) with arrow marks showing the sampling and measuring points at Nachikinskie hot springs (location ④) (N), area in Central Kamchatka (12 [th], October, 2002). N 1 ; General view of the hot spring pool (1) and profusely formed black microbial mats (2). N 2 ; White (1 and 2) and yellow (3) hard particles covered on the tubewell used for lifting groundwater around the hot spring pool (N 1). Sampling points are marked by arrows.

4. Results and Discussion

4.1.1. Characteristics of hot springs water measured in the field

The water quality (pH, Eh, EC, DO, and WT) and elemental concentration for Mg, Ca, Mn, total Fe, Fe^{2+}, As, Ag, and Au measured in the field is given in Table 1. Water in all measuring points showed the neutral pH excepting a few. Alkalinity ranged between pH ; 7.7 and 9.1 in V 4, Ma, N 1, and N 2. While the acidic (pH ; 3.6) character was found at least in one point (M 3). Eh also showed the reductive (Eh ; -10〜 -350 mV) condition in almost all the water samples, while only 2 points (V 4 and V 5-top) indicated a little different (Eh ; 130 and 100 mV). A significantly higher EC (EC ; 1.01〜1.78 mS/cm) was observed in all the sampling points excepting Mutnovskie (M) and Malkinskie (Ma). They were ranging between 0.08〜0.57 mS/cm. Besides this, dissolved oxygen (DO) and water temperature (WT) were found ranging between 0.5〜4.5 mg/l and 35〜91 ℃, respectively.

In addition, pack-test results showed the more or less concentration of elements (Mg, Ca, Mn, total Fe, Fe^{2+}, As, and Ag), exception of Au in all water samples. It was noted that the high concentration of As (0.2〜2.0 ppm) was found corresponding to that of iron (0.2 〜10.0 ppm) in most of the samples. Not only that but also As showed some correlation with Ca and Ag as Fe was absent in few points (Ma and N 2).

Table 1. Characteristics of hot spring waters for Kamchatka, Russia.

Measuring points			pH	Eh (mV)	EC (mS/cm)	DO (mg/l)	WT (℃)	Elements : pack test (ppm)							
								Mg	Ca	Mn	Total Fe	Fe^{2+}	As	Ag	Au
①	Vilyuchinskie	V1	6.7	-90	1.61	2.0	62	N.A.	N.A.	N.A.	N.A.	N.A.	N.A.	N.A.	N.A.
		V2	6.7	40	1.17	1.9	38	N.A.	N.A.	N.A.	N.A.	N.A.	N.A.	N.A.	N.A.
		V3	6.7	-210	1.59	1.6	53	N.A.	N.A.	N.A.	N.A.	N.A.	N.A.	N.A.	N.A.
		V4	8.2	130	1.01	4.5	35	N.A.	N.A.	N.A.	N.A.	N.A.	N.A.	N.A.	N.A.
		V5 top	7.4	100	1.47	3.4	42	N.A.	N.A.	N.A.	N.A.	N.A.	N.A.	N.A.	N.A.
		V5 bottom	7.3	-40	1.41	3.8	42	2.0	15.0	<0.5	0.2	0.2	<0.2	0.5	-
		V5 side	6.5	-10	1.50	0.5	55	2.0	15.0	<0.5	1.0-2.0	0.5-1	0.5	0.3-0.5	-
		V6	6.5	-20	1.51	0.7	48	2.0	15.0	0.5	1.0-2.0	1.0	1.5	0.5	-
②	Mutnovskie	M2	6.7	-280	0.57	4.0	65	5.0-10.0	20.0	0.5	-	-	0.2-0.5	-	-
		M3	3.6	-50	0.43	1.9	91	1.0-2.0	>50.0	0.5	>10.0	>10.0	-	-	-
③	Malkinskie	Ma	9.1	-350	0.08	2.3	68	tr.	2.0	-	-	-	1.0-2.0	0.5	-
④	Nachikinskie	N1	8.1	-160	1.70	2.3	58	<1.0	5.0-10.0	-	-	-	-	0.5-1.0	-
		N2	7.7	-330	1.78	0.8	79	tr.	10.0	-	-	-	0.5	0.5	-

tr. ; Trace, - ; Not detected, N.A. ; Not Analysed

4.1.2. γ-ray analysis around the sampling points in the fields

The γ-ray value around the sampling points in the fields is given in Table 2. The total γ-ray value (measured by spectrosurvey meter) of all measuring points were found ranging between 0.035～0.134 μSv/h. Especially, the total γ-ray value of Vilyuchinskie hot springs showed the higher (0.076～0.134 μSv/h) than those of Mutnovskie (0.069 and 0.083 μSv/h), Malkinskie (0.035 μSv/h), and Nachikinskie (0.076 and 0.077 μSv/h). Furthermore, the other types of γ-ray counter (Radi) also showed the higher value of γ-ray in all sampling points of Vilyuchinskie hot springs than others. The energy levels of 130～150 keV and 320～380 keV were found higher γ-ray values (μSv/h) in all the sampling points than those of 450～550 keV, 610～710 keV, 1150～1350 keV, or 1350～1500 keV.

Table 2. γ-ray analyses around the sampling points at Kamchatka, Russia. (μSv/h)

Measuring points			130 ～ 150keV (^{141}Ce)	320 ～ 380keV (^{131}I)	450 ～ 550keV (^{103}Ru)	610 ～ 710keV (^{137}Cs)	1150 ～ 1350keV (^{60}Co)	1350 ～ 1500keV (^{40}K)	Total*	Total**
①	Vilyuchinskie	V1	N.A.	N.A.	N.A.	N.A.	N.A.	N.A.	N.A.	0.131
		V2	N.A.	N.A.	N.A.	N.A.	N.A.	N.A.	N.A.	0.079
		V3	0.070	0.170	0.020	0.020	0.010	0.004	0.100	N.A.
		V4	N.A.	N.A.	N.A.	N.A.	N.A.	N.A.	N.A.	N.A.
		top	0.055	0.122	0.012	0.012	0.007	0.003	0.076	0.027
	V5 bottom	0.122	0.210	0.027	0.022	0.013	0.004	0.134	0.037
		side	0.158	0.143	0.014	0.018	0.009	0.004	0.097	0.062
		V6	0.081	0.139	0.015	0.014	0.008	0.004	0.090	0.038
②	Mutnovskie	M2	0.071	0.116	0.012	0.012	0.008	0.003	0.083	0.043
		M3	0.073	0.094	0.011	0.009	0.006	0.003	0.069	N.A.
③	Malkinskie	Ma	0.054	0.034	0.004	0.006	0.003	0.001	0.035	N.A.
④	Nachikinskie	N1	0.086	0.100	0.009	0.012	0.009	0.004	0.076	0.033
		N2	0.053	0.107	0.012	0.013	0.009	0.004	0.077	N.A.

N.A. ; Not Analysed
* ; total value by spectrosurvey meter
** ; total value by Radi

4.2. Chemical and mineralogical analyses of microbial mats and sediments collected from hot springs

The results of Energy dispersive X-ray fluorescence (ED-XRF) and X-ray powder diffraction (XRD) analyses are given in Table 3.

4.2.1. Vilyuchinskie hot springs (V)

The ED-XRF analysis of red microbial mats (V 1, V 3, V 5-6, and V 6-1) showed the high concentration of Ca, with Si, Fe, Mn, and traces of Mg, Al, S, As, and Sr. Whereas, the XRD results of same microbial mats showed the diffraction pattern of calcite (3.04, 2.29, and 2.10 Å) and amorphous Fe (2.5 Å), with aragonite (3.40, 3.20, and 2.71 Å) found

only in the point V 1. It was noted that a very high concentration of As was found in V 3, V 5-6, and V 6-1. Seemingly, there was correlation with that of high Fe concentration. Green microbial mats (V 2, V 5-1, V 5-3, V 5-5) also indicated high concentration of Ca with traces of Mn, Si, P, S, K, As, and Sr. While XRD patterns confirmed the presence of calcite and aragonite minerals (Fig. 7). Black microbial mats (V 4, V 5-2, V 5-4) showed high concentration of Ca associated with Mn, Mg, Al, Si, P, K, Fe, As, and Sr. The pattern of XRD indicated the presence of calcite and aragonite minerals as well. Besides this, Si, Fe, and Al were detected in the only sediment collected from V 6-2, which indicated noticeable diffraction peaks of smectite clay minerals (16 Å), feldspars (3.18, 3.23, and 3.75 Å) and siderite (2.83 and 1.71 Å).

4.2.2. Mutnovskie hot springs (M)

The ED-XRF analysis of clay sediment (M 1-1) showed concentrations of Si, Al, and Fe with the traces of S, Mg, P, K, Ca, Ti, Cr, Mn, Cu, Zn, and Zr. The XRD pattern showed the different diffraction consisting mainly of kaolin clay minerals (7.0 Å), zeolite (8.96 and 3.9 Å), hematite (2.69, 2.51, and 3.6 Å), and pyrite (2.71, 1.6, and 2.4 Å) (Fig. 7). White microbial mats (M 2-1) contained high concentration of S associated with traces of Mg, Al, Si, K, Ca, Mn, and Fe, whereas XRD pattern showed the diffraction of sulfur minerals (3.85, 3.21, and 3.44 Å) only. Green and gray microbial mats (M 2-2, M 2-3) also indicated high concentration of Si associated with Al, S, K, Ti, Mn, Fe, and Sr, while Na, P, Cr were only found in the green microbial mats. Both samples indicated diffraction peaks of smectite clay minerals and quartz (3.34, 4.26, and 1.82 Å), kaoline clay minerals, zeolite, calcite and ferrihydrite (2.52, 1.93, and 2.27 Å). Whereas, the XRD patterns of gray microbial mats showed the presence of smectite, clinoptiolite (8.83, 3.96, and 2.96 Å), feldspars, and pyrite. Furthermore, brown sediment (M 3-1) contained Fe, Si, and Al with the traces of Mg, P, S, K, Ca, Ti, Mn, Cu, and Sr. The XRD patterns showed the diffraction patterns of hematite, goethite, ferrihydrite, feldspars, and cristobalite (4.04, 2.49, and 2.84 Å) (Fig. 7). It was suggested that the concentration of Fe might originate from iron minerals. Additionally, white sediment (M 3-2) contained high concentration of S with the traces of Al, Si, K, Ca, and Fe, designated by the high peak of sulfur minerals (Fig. 7).

4.2.3. Malkinskie hot springs (Ma)

ED-XRF results of all microbial mats (Ma-1, Ma-2, Ma-3, Ma-4, and Ma-6) showed the similar chemical composition among them. They comprised Si, Ca, and Fe associated with Mg, Al, P, S, K, Ti, Mn, and Sr. XRD pattern of these microbial mats showed the same tendency towards the strong peaks of quartz, feldspars, smectite clay minerals, and cristobalite. Additionally, a broad peak was found that indicated the existence of ferrihydrite. The white microbial mats (Ma-5) comprised a high concentration of Si with the traces of Al, P, Ca, Ti, Mn, and Fe, and XRD patterns confirmed the presence of amorphous materials.

Table 3. Energy dispersive X-ray fluorescence (ED-XRF) and X-ray powder diffraction (XRD) analyses of sediments and biomats collected from Vilyuchinskie, Mutnovskie, Malkinskie and Nachikinskie hot springs.

Sampling points			Na	Mg	Al	Si	P	S	Cl	K	Ca	Ti	Cr
①	Vilyuchinskie	V1	-	0.21	0.34	4.33	-	0.37	-	-	85.03	-	-
		V2	-	-	-	0.79	0.56	1.28	-	0.13	94.56	-	-
		V3	-	0.25	-	27.91	-	0.04	-	0.09	5.15	-	-
		V4	-	0.36	0.59	3.22	0.75	1.36	-	0.03	87.70	-	-
		V5-1	-	0.56	0.49	5.29	1.25	2.11	-	1.71	57.78	-	-
		V5-2	-	-	0.58	3.30	0.21	1.26	-	0.06	88.44	-	-
		V5-3	-	0.47	0.32	6.42	0.90	1.22	-	0.86	45.37	-	-
		V5-4	-	0.36	0.73	4.18	0.26	1.28	-	-	84.29	-	-
		V5-5	-	-	0.29	10.54	0.24	0.78	-	0.20	48.19	-	-
		V5-6	-	-	0.84	14.82	0.44	0.25	-	0.08	23.28	-	-
		V6-1	-	-	1.52	19.87	-	0.28	-	0.33	10.62	0.16	-
		V6-2	-	0.28	11.14	49.25	0.74	0.52	-	1.52	5.44	1.21	-
②	Mutnovskie	M1-1	-	1.02	27.47	42.79	0.21	10.40	-	0.59	0.54	0.91	0.01
		M2-1	-	0.17	0.44	1.96	-	96.47	-	0.11	0.39	-	-
		M2-2	0.62	1.71	10.06	37.84	2.29	4.60	-	2.57	26.24	1.27	0.04
		M2-3	-	1.56	13.90	57.28	-	4.66	-	3.59	9.50	1.24	-
		M3-1	-	2.83	12.66	28.68	0.44	1.45	-	0.85	5.02	1.48	-
		M3-2	-	-	5.96	2.81	-	82.75	-	0.05	0.13	-	-
③	Malkinskie	Ma-1	-	4.98	6.12	32.60	5.70	6.77	-	6.44	15.72	1.49	-
		Ma-2	2.77	8.71	9.75	44.56	1.95	2.10	-	3.46	9.60	1.40	-
		Ma-3	2.48	5.80	9.61	42.52	1.88	2.21	-	3.82	15.10	1.40	-
		Ma-4	2.94	7.19	11.36	48.44	1.00	0.70	-	2.76	7.15	1.30	-
		Ma-5	-	-	0.55	85.67	2.55	-	-	-	7.46	0.39	-
		Ma-6	3.55	6.63	10.91	48.81	1.02	1.50	-	2.42	7.19	1.24	-
④	Nachikinskie	N1-1	3.79	2.02	14.06	54.67	0.77	0.65	-	3.59	7.65	1.37	-
		N1-2	3.59	1.76	12.96	55.35	-	0.90	-	3.14	7.81	1.25	-
		N2-1	8.18	-	-	7.39	-	25.15	6.29	6.48	12.56	-	-
		N2-2	15.30	-	-	39.75	-	9.08	16.31	0.83	10.79	-	0.02
		N2-3	37.02	-	0.94	4.75	-	45.83	-	0.09	8.02	0.10	-

The ED-XRF (wt%) header spans columns Na through Cr.

- ; Not Detected

4.2.4. Nachikinskie hot springs (N)

ED-XRF result of black microbial mats (N 1-2) indicated concentration of Si associated with the traces of Na, Mg, Al, S, K, Ca, Ti, Mn, Fe, As, and Sr. While XRD pattern showed the diffraction patterns of smectite, quarts, and feldspars. Beside this, clayey sediments (N 1-1) have the same tendency as elemental composition. Additionally, two different elements, namely P and Zn were present, while As was absent in it (Fig. 7). Furthermore, ivory white sediment (N 2-2) mainly contained Si, Cl, Ca, and Na with the S, K, Cr, Mn, Fe, As, Sr, and Cd. The XRD results of this sediment showed the strong diffraction

ED-XRF (wt%)									XRD
Mn	Fe	Cu	Zn	As	Sr	Zr	Cd	Ba	Detected minerals
2.34	6.48	-	-	0.76	0.14	-	-	-	Cc+Ara
2.41	-	-	-	0.10	0.16	-	-	-	Cc
0.40	63.27	-	-	2.83	0.06	-	-	-	Cc+Amorphous Fe
2.37	3.43	-	-	0.13	0.06	-	-	-	Cc+Ara
1.36	25.21	-	-	1.89	0.31	-	-	2.04	Cc+Ara
2.71	3.03	-	-	0.21	0.20	-	-	-	Cc+Ara
1.40	37.63	-	-	4.64	0.24	-	-	0.53	Cc+Ara
3.12	5.24	-	-	0.32	0.21	-	-	-	Cc+Ara
5.14	30.28	-	-	4.18	0.15	-	-	-	Cc+Qz
0.74	51.15	-	-	8.40	-	-	-	-	Cc+Amorphous Fe
0.66	58.26	-	-	8.22	0.09	-	-	-	Cc+Amorphous Fe
0.39	29.16	-	-	0.25	0.10	-	-	-	Sme+Fd+Sd
0.28	15.69	0.01	0.06	-	-	0.02	-	-	Kao+Ze+He+Py
0.02	0.44	-	-	-	-	-	-	-	Sulfur
1.55	11.11	-	-	-	0.11	-	-	-	Sme+Kao+Ze+Qz+Cc+Fh
0.28	7.89	-	-	-	0.12	-	-	-	Sme+Cp+Qz+Fd+Py
0.43	46.09	0.04	-	-	0.04	-	-	-	Fd+Ct+He+Gt+Fh
-	8.28	-	-	-	-	-	-	-	Sulfur
0.64	19.35	-	-	-	0.19	-	-	-	Sme+Kao+Qz+Ct+Fd+Fh
0.58	14.98	-	0.05	-	0.09	-	-	-	Sme+Kao+Qz+Ct+Fd+Fh
0.61	14.48	-	0.04	-	0.05	-	-	-	Sme+Kao+Qz+Ct+Fd+Cc+Fh
0.54	16.42	0.03	0.07	-	0.10	-	-	-	Sme+Kao+Qz+Ct+Fd+Fh
0.15	3.22	-	-	-	-	-	-	-	Amorphous materials
0.56	16.12	-	-	-	0.05	-	-	-	Sme+Qz+Fd+Mt
0.28	10.84	-	0.02	-	0.30	-	-	-	Sme+Mica+Kao+Qz+Fd+Px+Ze+Ct
0.54	12.45	-	-	0.04	0.21	-	-	-	Sme+Qz+Fd
0.30	33.23	-	-	-	0.42	-	-	-	Gy+Jt
0.18	6.53	-	-	0.04	0.45	-	0.71	-	Gy+Td+Qz
-	0.99	-	-	0.01	0.09	-	2.18	-	Hl+Cc+Py+Sulfur

Ara;Aragonite, Cc;Calcite, Cp;Clinoptilolite, Ct;Cristobalite, Fd;Feldspars, Fh;Ferrihydrite, Gt;Goethite, Gy;Gypsum, He;Hematite, Hl;Halite, Jt;Jarosite, Kao;Kaolin clay minerals, Mica;Mica clay minerals, Mt;Magnetite, Px;Pyroxene, Py;Pyrite, Qz;Quartz, Sd;siderite, Sme;Smectite, Td;Thenardite, Ze;Zeolite.

peaks of thenardite (2.78, 3.18, and 3.08 Å), gypsum, and quarts (Fig. 7). It was suggested that Na and S might originate from thenardite. The ED-XRF analysis of white sediments (N 2-3) showed the high concentration of S and Na associated with Al, Si, K, Ca, Ti, Fe, As, Sr, and Cd. The XRD results of white sediments showed the diffraction pattern of halite (2.82, 1.99, and 1.62 Å), calcite, pylite, and sulfur mineral. The high concentration of S might originate from pyrite. As well, high concentration of Na was responsible for halite.
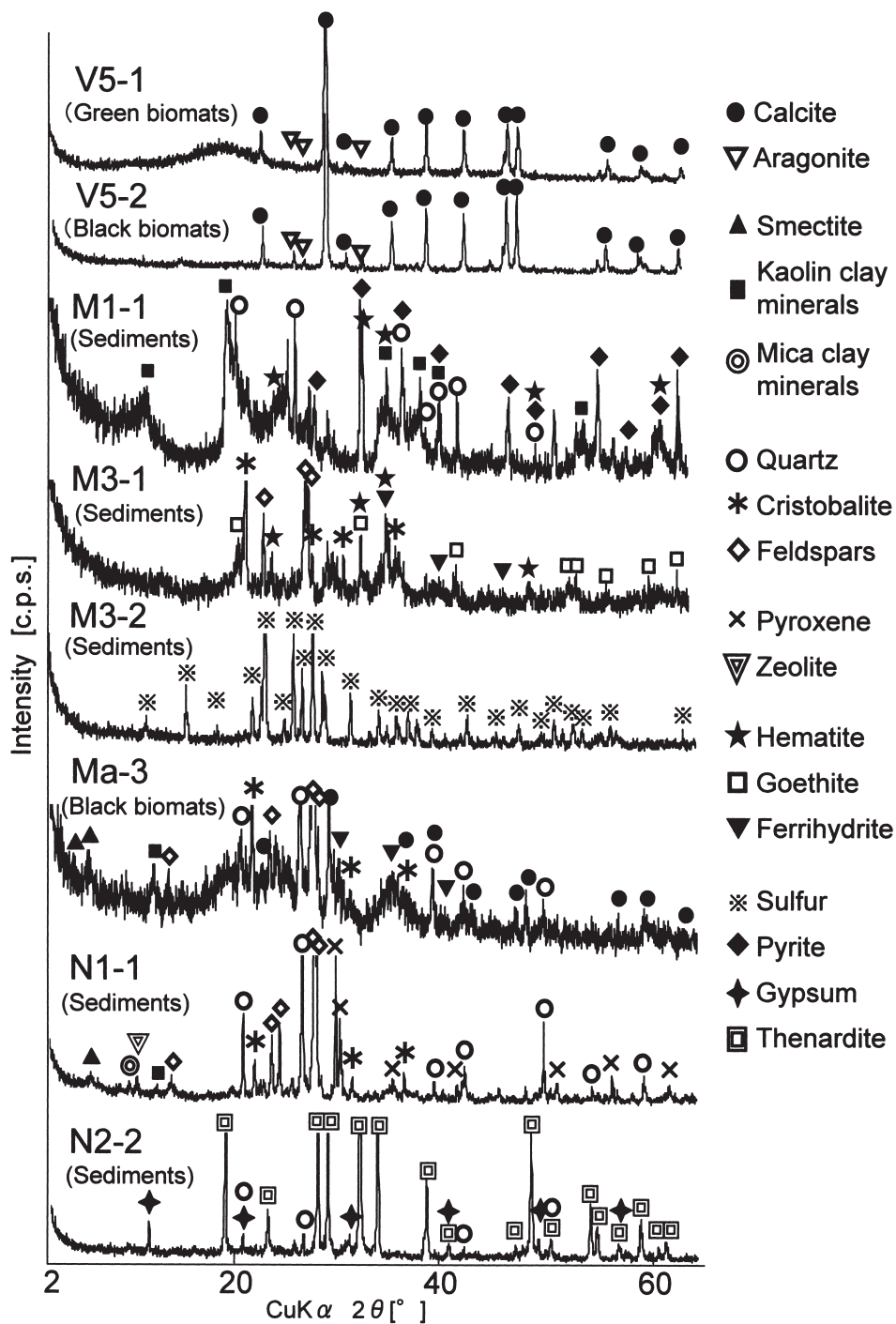
Fig. 7. XRD patterns of the representative sediments and microbial mats for each sampling site. Symbol with numbers correspond to those given in Fig. 2-6.

4.3. Fluorometric enumeration of bacteria in Vilyuchinskie hot springs water

The bacterial enumeration was conducted by using two kinds of fluorometric methods, that is, TBN (total bacteria number) and EAB (enzymatically active bacteria) at 4 sampling points of Vilyuchinskie hot springs. The points were V 3, V 5-side, V 5-bottom, and V 6. Points of V 3, V 5-side, and V 6 are natural hot springs, the other (V 5-bottom) is natural pond. The results are given in Table 4. The highest total bacteria number was found at sampling point V 5-bottom ($106.0 \pm 10.2 \times 10^3$ cells ml^{-1}), while the lowest one was $9.9 \pm 0.4 \times 10^3$ cells ml^{-1} found in sampling point V 5 - side. It was apparent that all hot springs possessed the similar tendency in population size of bacteria, i.e., the bacteria showed the population size of less than 10^5 cells ml^{-1} indicating a small number of bacteria. One possible reason for the low cell number of bacteria might be the high concentration of heavy metals such as As, Cr, and Sr in these springs. The heavy metallic concentration in these hot spring water is in agreement with some works of Okrugin *et al*. (1994), Chudaev *et al*. (2000) and Okrugin *et al*. (2002). The result suggests that these heavy metals might be toxic to bacteria.

Additionally, based on the enumeration of EAB, the highest fraction of EAB was 91 ± 3 % in the water of sampling point V 5 - side, whereas the lowest one was detected in sampling point V 5 - bottom (27 ± 3 %). In natural hot spring water showing low TBN, the fraction of active bacteria was high that indicates active participation of bacteria in biogeo-chemical reactions.

Table 4.   Total bacteria number and active bacteria enumeration in water samples from Vilyuchin-skie hot springs ① of Kamchatka, Russia.

Sampling points	Total cell counts ($\times 10^3$ ml^{-1}) (mean $\pm$ SD)*	Enzymatically active bacteria (EAB) counts ($\times 10^3$ ml^{-1}) (mean $\pm$ SD)	Fraction (%) of EAB cells (mean $\pm$ SD)**
V3	16.3 $\pm$ 1.5	7.5 $\pm$ 0.9	46 $\pm$ 7
V5-side	9.9 $\pm$ 0.4	8.9 $\pm$ 0.2	91 $\pm$ 3
V5-bottom	106.0 $\pm$ 10.2	28.2 $\pm$ 3.0	27 $\pm$ 3
V6	16.7 $\pm$ 1.6	10.7 $\pm$ 1.7	64 $\pm$ 5

* ; Mean and standard deviation (SD) were calculated from the counts of 10 to 20 randomly chosen fields on each filter,

** ; Percent detection compared to 4',6-diamidino-2-phenilindole (DAPI) fluorescence.

4.4. Microscopic observation and EDX analysis of microbial mats from Vilyuchinskie hot springs (V)

4.4.1. Microbial mats at point V 1

Reddish brown microbial mats (see Fig. 2) were mainly composed of brown mineral particles that are spherical in shape (Fig. 8 A). Epifluorescence micrographs revealed bacterial cells absorbed the fluorescent blue in DAPI-stained microbial mats (Fig. 8 B). This indicated that the reddish brown microbial mats contained granular materials with living bacteria. SEM micrograph of the same microbial mats showed the sheath of filamentous bacteria covered with mineral particles that are less than 0.5 µm in size (Fig. 8 C). Beside this, EDX spectrum indicated the high concentration of Ca associated with Mn, Si, Fe, and As on the rod-shaped bacteria (Fig. 8 C inset).

4.4.2. Microbial mats at point V 2

Optical micrographs of green-colored microbial mats (see Fig. 2) showed filamentous cyanobacteria and mineral particles of approximately 10 µm in size (Fig. 9 A, B). SEM observation recognized the cyanobacteria attached with mineral particles. On the other hand, EDX spectrum of cyanobacteria (arrow 1 in Fig. 9 C inset) showed the presence of Ca, Si, P, S, Cl, and Fe with a hilly back ground, suggesting the presence of organic materials. Mineral particles attached on cyanobacterial surface (arrow 2 in Fig. 9 C inset) were mainly composed of Si and Ca, with traces of S, Fe, and Mn.

4.4.3 Microbial mats at point V 3

Optical micrograph of brown microbial mats (see Fig. 2) showed the presence of high density brown-colored materials (Fig. 10 A). Epifluorescence micrograph showed spherical, rod-shaped and filamentous bacteria associated with brown-colored minerals (Fig. 10 B). SEM micrograph of brown microbial mats showed bacteria in long chains of approximately 5 µm in size associated with mineral particles (Fig. 10 C). The arrows in Fig. 10 C indicated analytical points of bacteria surface (arrow 1) and mineral particles (arrow 2). EDX spectra (Fig. 10 C inset) of arrow 1 and arrow 2 showed the presence of Si, Fe, and Ca, and chained bacterial surface containing the concentration of As more than that of mineral particles.

4.4.4. Microbial mats at point V 4

Optical micrograph of green microbial mats (see Fig. 2) showed filamentous cyanobacteria and mineral particles (Fig. 11 A). Algal and cyanobacterial cells had a red color indicating the presence of chlorophyll (Fig. 11 B). SEM micrographs of green microbial mats showed algal filamentous and mineral particles. The EDX spectra of mineral (arrow in Fig. 11 C) showed that they were mainly composed of Ca with the traces of P, S, and Si. It could be suggested that this mineral was calcite. The magnified view (Fig. 11 D) of arrow in Fig. 11 C revealed the presence of calcite minerals covered with biofilms.

4.4.5 Microbial mats at point V 5
Top part of point V 5 (arrow 1)

Green microbial mats (see Fig. 3) were mainly composed of short rod-shaped bacteria of 5 µm in size and chained bacteria of approximately 15 µm in size (Fig. 12 A). Both types of bacterial cells had red color indicating the chlorophyll content (Fig. 12 B). SEM micrograph of green microbial mats showed short rod-shaped bacteria (Fig. 12 C). As well, EDX spectrum (arrow in Fig. 12 C) indicated the presence of Ca, Si, P, S, Fe, and Ti with a hilly background.

Top part of point V 5 (arrow 2)

Black microbial mats (see Fig. 3) were mainly composed of filamentous cyanobacteria with mineral particles (Fig. 13 A). Filamentous cyanobacterial cells had red color indicating the chlorophyll content (Fig. 13 B). SEM micrograph of black microbial mats showed filamentous cyanobacteria with minerals (Fig. 13 C). Additionally, EDX spectrum (arrow in Fig. 13 C) indicated the high amount of Ca with traces of Si, P, S, Mn, and Fe.

Bottom part of point V 5 (arrow 3)

Green microbial mats (see Fig. 3) were mainly composed of short rod-shaped bacteria of around 5 µm in size together with mineral particles (Fig. 14 A). Short rod-shaped bacterial cells had red color indicating the chlorophyll content (Fig. 14 B). SEM micrograph of short rod-shaped bacteria showed the presence of minerals on it. Furthermore, EDX spectra of minerals that covered bacterial surface (arrow 1 in Fig. 14 C) showed the presence of Fe, Si, Al, Ca, P, S, and As, while the bacterial surface (arrow 2) showed the presence of Si, Fe, Al, Ca, P, and S. It was suggested that the bacteria might be capable of accumulating As.

Bottom part of point V 5 (arrow 4)

Black microbial mats (see Fig. 3) were mainly composed of filamentous cyanobacteria with the variety of mineral particles (Fig. 15 A). They showed the similarity with that of upper part. Epifluorescence micrograph showed only bacterial DNA in presence of blue coloration (Fig. 15 B). SEM micrograph and EDX spectrum of mineral showed a high amount of Ca associated with Al, Si, P, S, Mn, and Fe, suggesting the presence of Mn-contained calcite minerals (Fig. 15 C).

Side part of point V 5 (arrow 5)

Optical light micrograph of black microbial mats (see Fig. 3) showed brown mineral particles and filamentous cyanobacteria (Fig. 16 A). Epifluorescence micrograph showed a diversity of bacteria and filamentous cyanobacteria attached to mineral aggregates (Fig. 16 B). The cyanobacterial color is red indicating the chlorophyll content. SEM micrograph of filamentous bacteria and EDX spectra showed the presence of As in filamentous bacteria, covered with mineral capsule (Fig. 16 C).

Side part of point V 5 (arrow 6)

Optical light micrograph of reddish brown microbial mats (see Fig. 3) showed the high density brown materials (Fig. 17 A). Epifluorescence micrograph showed the abundance of rods-shaped bacteria of approximately 5 μm in size (Fig. 17 B). SEM micrograph and EDX spectrum of filamentous bacteria showed the presence of Al, Si, Ca, and Fe associated with As in mineral surrounding bacterial surface (Fig. 17 C).

4.4.6 Observation of microbial mats at point V 6

Optical micrographs (Fig. 18 A, B) of reddish brown microbial mats (see Fig. 3) showed the high density brown materials and filamentous cyanobacteria with spherical bacteria. SEM micrograph (Fig. 18 C) of filamentous bacteria in red microbial mats and EDX spectra showed the presence of Al, Si, Ca, and Fe associated with As in both bacteria cells and mineral particles.

4.5. Microscopic observation of microbial mats from Mutnovskie hot spring (M)
4.5.1 Observation of microbial mats at point M 2-1

Optical and scanning micrographs of white microbial mats (see Fig. 4) showed sulfur bacteria in white microbial mats (Fig. 19 A, B, and C). EDX spectra of analysed points arrow 1 and arrow 2 showed the S content in association with P and Fe in bacterial cells and the high concentration of S associated with Al, Si, P, K, Ca, and Fe in the particles (Fig. 19 C inset).

4.5.2 Observation of microbial mats at point M 2-2

Optical micrographs of black-colored microbial mats (see Fig. 4) showed filamentous cyanobacteria covered with black-colored mineral particles. A diversity of bacteria is detected by DAPI fluorescence in these black-colored particles (Fig. 20 A, B). SEM micrograph showed filamentous cyanobacteria and sulfur bacteria (Fig. 20 C). EDX spectra of filamentous cyanobacteria revealed the presence of Si, P, S, Ca, Mn and Fe. The cyanobacteria is rich in Mn on the cell wall (Fig. 20 C inset).

4.5.3. Observation of microbial mats at point M 2-3

Micrographs of grey colored microbial mats showed algae in association with mineral particles (Fig. 21 A, B, C). EDX spectra of analytical point arrow 1 showed the concentrations of Si, Al, and S associated with Ca and Fe, whereas mineral particles attached on algae were mainly composed of Si, Al, S, and Fe with the traces of Ca, P, K, and Ti (Fig. 21 C inset).

4.6. Microscopic observation of microbial mats from Malkinskie hot spring (Ma)
4.6.1. Observation of microbial mats at point Ma-1

Green microbial mats at point Ma-1 were mainly composed of cyanobacteria (Fig. 22

A, B). The cyanobacterial cells were approximately 5 μm in length, and they lived together in groups. EDX spectrum of filamentous bacteria showed the presence of P and S with trace of Ca (Fig. 22 C inset).

4.6.2. Observation of microbial mats at point Ma-2

Optical light (Fig. 23 A) and epifluorescence (Fig. 23 B) micrographs of orange microbial mats showed filamentous cyanobacteria associated with cocci, bacilli and filamentous bacteria. SEM micrograph of orange microbial mats showed Anabaena-typed cyanobacteria covered with thin film and filamentous cyanobacteria (Fig. 23 C). In addition, EDX spectrum indicated the presence of Si associated with Mg, Al, P, S, Ca, Mn, and Fe (Fig. 23 C inset).

4.6.3 Observation of microbial mats at point Ma-3

Optical light micrographs of black microbial mats showed the filamentous cyanobacteria attached with mineral particles (Fig. 24 A, B). The size of cyanobacterial cells were 25 μm in width. SEM micrograph and EDX spectrum of filamentous bacteria showed the high concentrations of S and Si with traces of Ca and Fe (Fig. 24 C).

4.6.4 Observation of microbial mats at point Ma-4

Optical light and epifluorescence micrographs of reddish brown microbial mats showed a diversity of cyanobacterial and bacterial cells formed colonization (Fig. 25 A, B). Cyanobacterial cells contained chlorophyll designated by the red color. It seemed clear that SEM micrograph showed the group of bacteria by producing slime layer. Additionally, EDX spectrum of short rods-shaped bacteria showed the high content of Si associated with Al, P, K, Ca, and Fe.

4.6.5. Observation of microbial mats at point Ma-5

Optical light (Fig. 26 A) and epifluorescence (Fig. 26 B) micrographs of white-colored microbial mats showed filamentous algae with sulfur bacteria. It was apparent that the sulfur bacteria attached to the filamentous algae by making a long chain with approximately 25 μm in distance. This was consistent with the SEM micrograph (Fig. 26 C). In addition, EDX spectra of sulfur bacteria and filamentous algae showed the high concentration of Si associated with P, Ca, and S. On the other hand, it was found that only filamentous algae contained Ca element.

4.6.6. Observation of microbial mats at point Ma-6

Optical micrographs showed colonization of spherical cyanobacteria associated with mineral particles (Fig. 27 A, B). SEM micrograph showed the colony of bacteria in coccus type predominantly (Fig. 27 C). Some of them existed covered with biofilm (arrow 3). Additionally, EDX spectra also confirmed that the coccus bacteria contained the high concen-

tration of Si and Al associated with P, S, Ca, Fe, and Mg. It was found that only one spherical bacterial cells (see arrow 2) contained high concentration of Ti element.

4.7. Microscopic observation of microbial mats from Nachikinskie hot springs (N)

Optical micrographs of black microbial mats at point N 1-2 showed filamentous cyanobacterial cells attached with mineral particles (Fig. 28 A, B). Besides that, SEM micrograph also revealed the presence of cyanobacteria with mineral particles. Based on the EDX spectra, it was found that the filamentous bacteria contained the high concentration of S and Ca associated with Si and P, while the mineral particles contained the high concentration of Si associated with Fe only.